Journal of Biomedical Optics

SPIEDigitalLibrary.org/jbo

Hyperspectral fluorescence imaging for cellular iron mapping in the *in vitro* model of Parkinson's disease

Eung Seok Oh
Chaejeong Heo
Ji Seon Kim
Minah Suh
Young Hee Lee
Jong-Min Kim

SPIE

Hyperspectral fluorescence imaging for cellular iron mapping in the *in vitro* model of Parkinson's disease

Eung Seok Oh,[a,b*] Chaejeong Heo,[c,d*] Ji Seon Kim,[e] Minah Suh,[c,f] Young Hee Lee,[d] and Jong-Min Kim[b]
[a]Chungnam National University Hospital, Chungnam National University School of Medicine, Department of Neurology, Daejeon, 301-721, Republic of Korea
[b]Seoul National University Bundang Hospital, Department of Neurology, Seongnam, Kyeonggi-do, 463-707, Republic of Korea
[c]Sungkyunkwan University, IBS Center for Neuroscience Imaging Research (CNIR), Suwon, Kyeonggi-do 440-746, Republic of Korea
[d]Sungkyunkwan University, IBS Center for Integrated Nanostructure Physics(CINAP), Suwon, Kyeonggi-do, 440-746, Republic of Korea
[e]Chungbuk National University Hospital, Department of Neurology, Cheongju, Republic of Korea
[f]Sungkyunkwan University, Department of Biological Science, Suwon, Kyeonggi-do, 440-746, Republic of Korea

Abstract. Parkinson's disease (PD) is characterized by progressive dopaminergic cell loss in the substantia nigra (SN) and elevated iron levels demonstrated by autopsy. Direct visualization of iron with live imaging techniques has not yet been successful. The aim of this study is to visualize and quantify the distribution of cellular iron using an intrinsic iron hyperspectral fluorescence signal. The 1-methyl-4-phenylpyridinium (MPP+)-induced cellular model of PD was established in SHSY5Y cells exposed to iron with ferric ammonium citrate (FAC, 100 μM). The hyperspectral fluorescence signal of iron was examined using a high-resolution dark-field optical microscope system with signal absorption for the visible/near infrared spectral range. The 6-h group showed heavy cellular iron deposition compared with the 1-h group. The cellular iron was dispersed in a small particulate form, whereas the extracellular iron was aggregated. In addition, iron particles were found to be concentrated on the cell membrane/edge of shrunken cells. The iron accumulation readily occurred in MPP+-induced cells, which is consistent with previous studies demonstrating elevated iron levels in the SN. This direct iron imaging could be applied to analyze the physiological role of iron, and its application might be expanded to various neurological disorders involving metals, such as copper, manganese, or zinc. [DOI: 10.1117/1.JBO.19.5.051207]

Keywords: high-resolution dark-field optical microscope; hyperspectral fluorescence signal; cellular iron; neuronal cell; Parkinson's disease.

Paper 130555SSPR received Aug. 1, 2013; revised manuscript received Oct. 9, 2013; accepted for publication Oct. 28, 2013; published online Dec. 2, 2013.

1 Introduction

Iron acts as an essential cofactor in many cellular functions of the central nervous system, such as DNA synthesis, the mitochondrial electron transport system, and neurotransmission.[1] During normal aging, iron accumulates in various brain areas, with especially high concentration in the structures of the globus pallidus, red nucleus, dentate nucleus, and substantia nigra (SN).[2] It is not certain yet why iron is selectively accumulated in these areas in a nonuniform manner. Dopaminergic neurons are located in a subarea of the SN and the pars compacta. Progressive loss of these neurons is a pathological hallmark of Parkinson's disease (PD), together with abnormally high deposition of iron in this area.[3] The elevated iron level in the SN of PD has been demonstrated by autopsy,[2] with 7-Tesla magnetic resonance imaging,[4] and by transcranial sonography.[5] The abnormal accumulation of iron may be associated with oxidative stress,[6] and imbalance of mechanisms controlling iron homeostasis may have a causal influence on the pathogenesis of PD.[7] The iron is changed in the brain between ferrous (Fe^{2+}) and ferric (Fe^{3+}) states via electron exchange process. The accumulated irons participate in the fenton reaction with hydrogen peroxide and bring about oxidative stress through the reactive oxygen species (ROS). Both neuromelanin and synthetic dopamine-melanin are bound to iron with a high degree and act as a strong iron chelator and scavenger of cytoplasmic iron.[8] Dopaminergic cells in the SN and ventral tegmental areas might be vulnerable to oxidative stress and selectively involved in this manner. Then the degree of oxidative stress in the iron-laden dopaminergic cells might be various depending on the location of iron in the nucleus, mitochondria, and other cytosolic organelles. Specific neurotoxin is used for the cellular model of PD *in vitro*. 1-Methyl-4-phenyl-1,2,3,6-tetrahydropyridine is a potent neurotoxin, converted by monoamine oxidase type B to the 1-methyl-4-phenylpyridinium (MPP+) in the brain. MPP+ is moved into the cell via dopamine transporter, particularly concentrated into mitochondria and therefore induces significantly decreased mitochondrial complex-I activity. Through this process, the depletion of ATP and increasing of reactive oxygen species (ROS) linking iron induces selective cell death of dopaminergic neurons.[9] To elucidate the role of iron as a potential cause of PD, understanding the distribution and quantification of cellular iron is essential. However, the extremely low concentration of iron in the cell is difficult to detect and to quantify by existing microscopy. Most previous quantification

*These authors contributed equally.

Address all correspondence to: Young Hee Lee, Sungkyunkwan University, IBS Center for Integrated Nanostructure Physics (CINAP), Suwon 440-746, Republic of Korea. Tel: 82-31-299-6507; Fax: 82-31-299-6505; E-mail: leeyoung@skku.edu; and Jong-Min Kim, Seoul National University Bundang Hospital, Department of Neurology, Seongnam, Kyeonggi-do 463-707, Republic of Korea. Tel: 82-31-787-7465; Fax: 82-31-787-4059; E-mail: jongmin1@snu.ac.kr

studies depended on the colorimetric ferrozine-based assay using cell lysates.[10,11] With a matter of concern, cellular iron level is influenced by microscopic changes in temperature or pH and may be changed by the physiological state of the cells with various chemicals.[11] Moreover, the previous methods have limitations to observe the location of iron and have difficulty analyzing the amount of iron in the intracellular organelles. An analytical technique with high-resolution imaging is needed for the visualization and quantification of cellular iron elevation as the pathology of PD progresses.

Conventional optical microscopy, with its large field-of-view and easy accessibility, is a popular choice for observing cells and tissues in biological experiments. Conventional optical microscopy has a near submicron range of spatial resolution (SR) by visible light,[12] but this resolution is not sufficient to image cellular iron. In this paper, we introduce a cellular iron imaging technique with a nanoscale SR optical microscope (SR < 100 nm) which does not require staining or chemical modification as with ferrozine. To observe the localized cellular iron and perform direct quantification without cell lysis or a staining method, we used a visible/near infrared (VNIR) hyperspectral fluorescence signal imaging system with a high-resolution dark-field optical condenser.[13] This nanoscale optical hyperspectral imaging system is different from the conventional optical microscope with regard to SR and spectral absorption techniques. The SR is 40–90 nm by metal halide light, which is a relatively high SR compared to that of a conventional optical microscope. For instance, it has been used to image quantum dots[14] and the interaction and uptake of nanoparticles in cells and tissues.[15,16] The hyperspectral imager absorbs the intrinsic fluorescence signal from the iron in the VNIR spectral range. This signal is scanned and mapped onto the cell image collected under the dark-field optical microscope. Because of the large field-of-view with high SR, we were able to image and map a large number of cells at one time—a procedure that is not possible with X-ray fluorescence (XRF) microscopy.[17,18] In this study, we introduced high-resolution dark-field optical microscopy to directly observe the VNIR hyperspectral fluorescence signal of cellular iron in a cellular model of PD.[13]

2 Materials and Methods

2.1 *Cell Culture*

Human neuroblastoma dopaminergic cells (SHSY5Y; ATCC, Virginia) were grown in Dulbecco's modified Eagle's medium (DMEM; Invitrogen, New York) supplemented with 10% heat-inactivated fetal bovine serum (FBS; Sigma-Aldrich, Missouri) and 1% penicillin-streptomycin (Invitrogen, New York) in a T75 flask at 37°C and 5% CO_2 in an incubator. The cells were incubated in serum-free conditioning medium and were treated with 300 μM of MPP+ for 24 h in the model of PD. MPP+-induced PD cells were treated with 100 μM of FAC (ferric ammonium citrate, Sigma-Aldrich, Missouri) for either 1 or 6 h to induce iron deposition. Each cell preparation was then washed three times with 1 ml of PBS. The cells were seeded on a cover glass coated with laminin (Roche Diagnostics GmbH, Mannheim, Germany) and grown in a 12-well plate in a 5% CO_2 incubator.

2.2 *Sample Preparation*

The neural cells on cover glass were fixed for 20 min with a 4% paraformaldehyde solution (Biosesang, Seongnam, South Korea) and rinsed three times with PBS at room temperature. The cells were mounted on a slide using mounting medium (Dako Cytomation, California). The samples were stored at 4°C before imaging.

2.3 *Imaging*

A hyperspectral nanoscale optical imaging system was assembled with a VNIR spectral range hyperspectral imager (CytoViva, Inc., Alabama), a high-resolution dark-field condenser (Numerical Aperture; NA = 1.2 – 1.4; CytoViva, Inc., Alabama) and an illuminator system (metal halide light; Welch Allyn Inc., New York) on an Olympus microscope (BX-53, Japan). The construct diagram of imaging system is shown in Fig. 1(a). This system provided ~90 nm resolution with an improved contrast and signal-to-noise ratio.[13] The

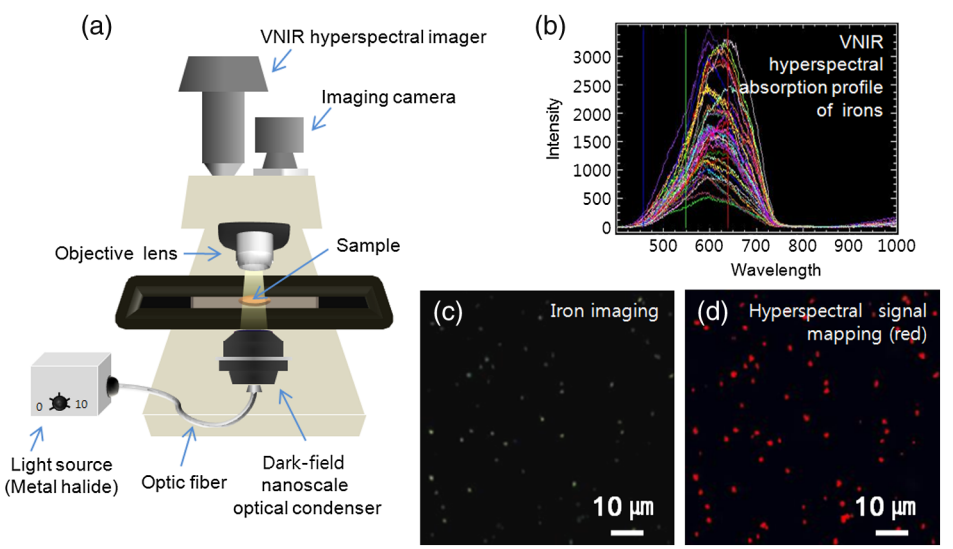

Fig. 1 Hyperspectral fluorescence signals and mapping images of iron [ferric ammonium citrate (FAC)] dispersed in water. (a) A schematic of the hyperspectral imaging system with visible/near infrared (VNIR) spectral range. (b) VNIR hyperspectral absorption profile of iron. (c) High-resolution optical image of iron with a dark-field nanoscale optical condenser. (d) The mapped hyperspectral signal is shown in red. Almost all points are identically mapped with the iron deposits shown in (c).

high-resolution dark-field condenser was directly positioned on the slide glass upon the workstage with the immersion solution and focused until to get a donut ring type in pattern of light. The dark-field optical image of sample was acquired and then hyperspectral absorption signal was recorded in the same position of sample. The images in the slide were obtained and recorded with a CCD camera (Olympus Microsystems, BX-53, Japan).

2.4 *Data Analysis and Statistics*

Region of interest (ROI) of cells tracing and analysis of the hyperspectral absorption signal were performed using CytoViva imaging software and Olympus microscope software (BX-53, Japan). Statistical evaluation was performed using an independent *t*-test (SPSS19, International Business Machines Corp., New York). Significant difference, *; p-value <0.1.

3 Results and Discussion

3.1 *High-Resolution Hyperspectral Optical Imaging in Cells*

We used the high-resolution dark-field imaging and hyperspectral fluorescence signal imaging system for the detection of cellular iron in a cellular model of PD. The imaging system has several compartments for high-resolution imaging up to the several nanometer range, which we have designated nanoscale resolution. These include a VNIR spectral range hyperspectral imager, a dark-field nanoscale optical condenser (numerical aperture; NA = 1.2–1.4), and a metal halide light illuminator [Fig. 1(a)]. This imaging system, which was developed by CytoViva, Inc., can visualize dark-field optical images of the sample and record the VNIR hyperspectral fluorescence signal absorption from the intrinsic signal. It can also visualize the fluorescence-tagged biosample. Using this system, we collected the fluorescence absorption signals from iron (FAC) to build a reference signal profile [Fig. 1(b)]. The signals showed peak absorption near 600 nm and varied in intensity; the intensity difference was due to the variable size of the iron aggregates. We also obtained the dark-field optical image of FAC iron [Fig. 1(c)]. This image was scanned with the reference signal, and then mapped in a red color [Fig. 1(d)]. The mapping results were highly correlated in Figs. 1(c) and 1(d).

We mapped the reference signal from the FAC iron deposits in water onto the dark-field image of cells treated with FAC [Fig. 2(a)]. The cells were prepared on a laminin-coated glass slide. The numerous extracellular iron aggregates (bulk iron) that were detected are shown in red color [Fig. 2(a)]. The hyperspectral fluorescence absorption signal profiles from the cells and iron deposits were compared in Fig. 2(b). Each square box was an ROI designated in Fig. 2(a). The extracellular bulk iron exhibited a very-high-intensity signal compared to the cell (cytoplasm, nucleus) or glass. The magnified images of the center of ROIs, including the high-intensity signal from the bulk iron, are shown in Fig. 2(c).

3.2 *Cellular Iron Imaging in PD Cell Model*

To investigate the distribution of cellular iron in the PD condition, we used the MPP+-induced SHSY5Y cells for an *in vitro* cell model of PD.[9] Cells were imaged as above, and the hyperspectral signal of iron was mapped in the cells conditioned using an MPP + /FAC treatment. We studied the variation in iron aggregation between a transient exposure (1 h) and a heavy exposure (6 h) to FAC. Figure 3 shows the hyperspectral mapping images of the cellular iron detected in the cells.

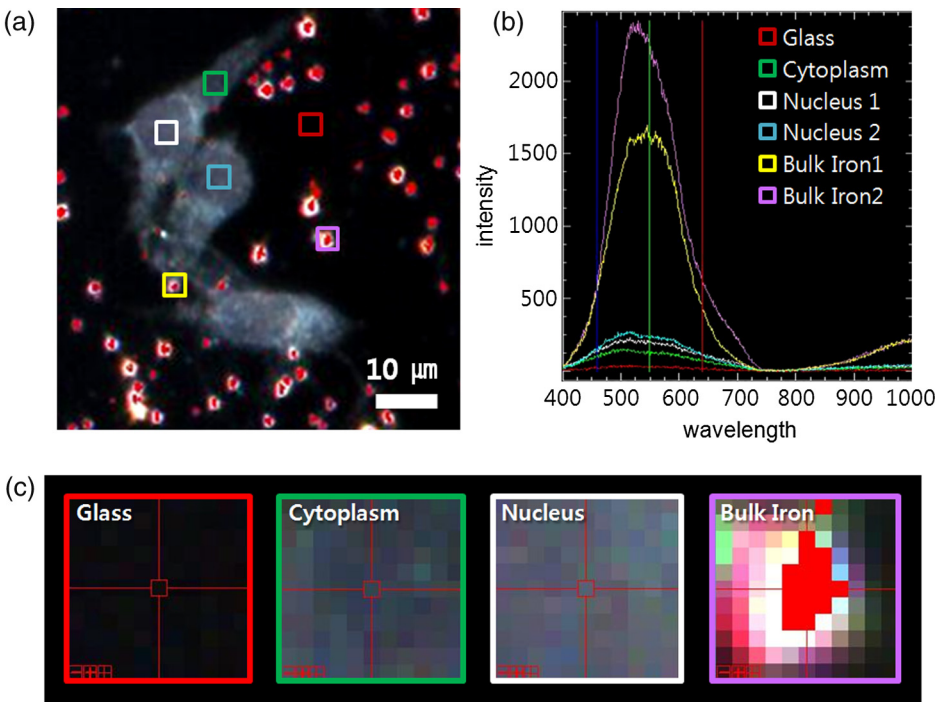

Fig. 2 Spectral profiles of different regions of the cells. (a) Dark-field images of the SHSY5Y cells [1-methyl-4-phenylpyridinium (MPP+)] incubated with FAC for 1 h, with the hyperspectral signal mapping areas marked by colored boxes. (b) The hyperspectral signal intensity of each area. All bulk iron areas have a peak absorbance near 600 nm, whereas the peak signal in the cells is near 500 nm and the signal on the glass plate is almost zero. (c) Magnified images (17×) of the hyperspectral fluorescence signal mapped from the glass, cytoplasm, nucleus, and bulk iron.

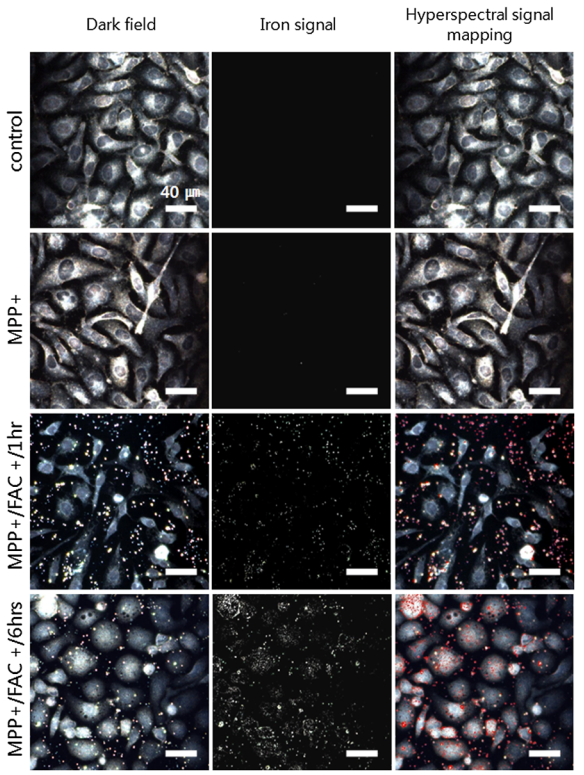

Fig. 3 Iron detection in the MPP+-induced Parkinson's disease (PD) cell model and the dependence of iron aggregation on the time of exposure. The dark field optical images (first row) and iron detection images (second row) in the SHSY5Y cells exposed with MPP+ only (without FAC) and with FAC for 1 or 6 h as a sign in right side. The hyperspectral iron signal on the mapping images indicated by red color (third row). All scale bars: 40 μm.

The magnified mapping images show the detailed cellular location of the iron (Fig. 4). Each cell was exposed to FAC for 1 h. The mapped location of iron was near the edge of most of the cells. Points a, b, c, d, and e are the yellow boxes in Figs. 4(a) and 4(b). The large bulk iron aggregates were dispersed in the extracellular area and several were detected on the cell surface. Many small particle-like iron deposits were located in the cells. Specifically, small iron clusters were found in the dendrites of cells, indicated by blue arrows in the images of d and e in Fig. 4.

In addition, we observed an even higher iron signal after 6-h exposure (Fig. 5). Dense iron deposits were detected in the MPP+-induced PD cells, and some of the cells shrank. The high iron accumulation was spread uniformly throughout individual cells and was found in most of the imaged cells [Figs. 5(a), 5(b), and 5(d)]. Locally deposited iron existed along the cell membrane of the shrunken cells [Figs. 5(a), 5(c), and 5(e)].

3.3 *Quantification of Cellular Iron in the Cellular Model of PD*

The hyperspectral signal intensity measurement of iron is easy for quantification method compare with routine iron measuring method of the colorimetric ferrozine-based assay.[10,11] Also, this hyperspectral signal imaging provides the location with quantity of iron which was not offered from colorimetric ferrozine-based assay. Using this intensity measurement, we can relatively quantify the intensity differences between sample groups without cell lysis (Fig. 6). To quantify the iron signal in single cells, the hyperspectral absorption intensity was analyzed for ROIs in each cell [Fig. 6(b) and 6(c)]. The ROI was excluded outside the area of cells. In Fig. 6, the average intensity for a single cell (total intensity for 20 cells) after 1 or 6 h of FAC exposure

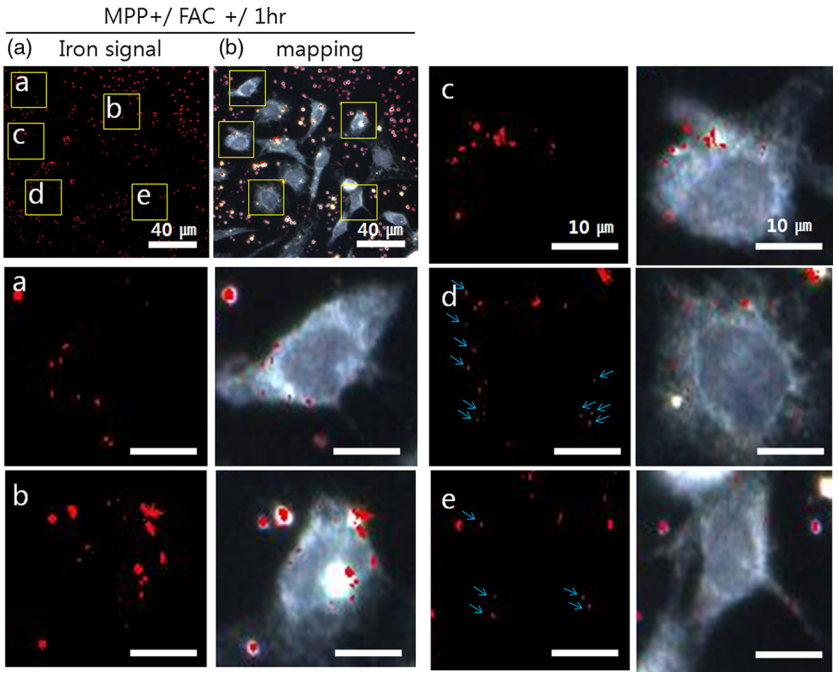

Fig. 4 Iron deposition in the MPP+-induced PD model after 1 h of exposure to FAC. The hyperspectral iron signals (a) were mapped onto the cell images (b) with red color. The magnified (4×) and representative images show in the points a, b, c, d, and e image set marked with yellow boxes in (a) and (b). Each a, b, c, d, and e image set has iron signal image (left) and mapped image on a cell (right). The blue arrows in d and e show very small particles. Scale bars (a and b): 40 μm. Scale bars (a, b, c, d, and e): 10 μm.

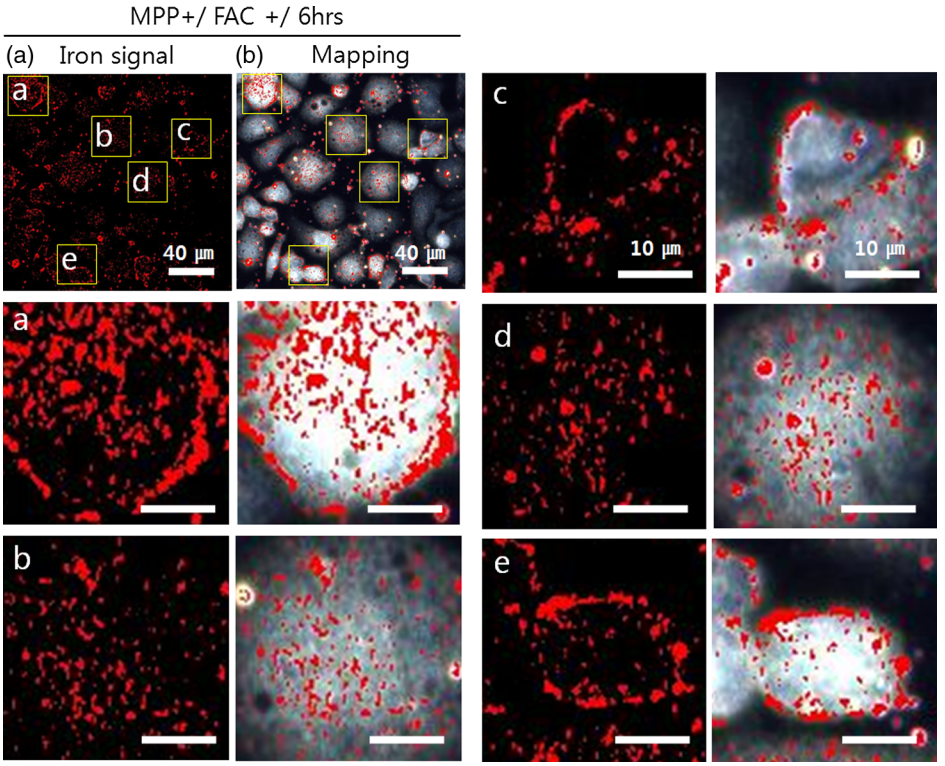

Fig. 5 Iron deposition in the MPP+-induced PD model after 6 h exposure to FAC. The hyperspectral iron signals (a) were mapped onto the cell images (b) with red color. The representative images of points a, b, c, d, and e show the magnified images (4×) from the yellow boxes in (a) and (b). Scale bars (a and b): 40 μm. Scale bars (a, b, c, d, and e): 10 μm.

was 198.6 a.u. (3973 a.u.) and 278.6 a.u. (5572 a.u.), respectively. The 6-h group showed statistically high cellular iron deposition compared with little accumulation in the 1-h group.

Cellular iron was dispersed in a small, particulate form, whereas the extracellular iron was detected in an aggregated form. Additionally, iron particles were found to be concentrated around the edge of the cell membranes of shrunken cells. Cellular iron accumulation was easily triggered in MPP+-induced cells, mirroring the previous studies and demonstrating the elevated iron levels in the SN of PD.[2–7,9,19]

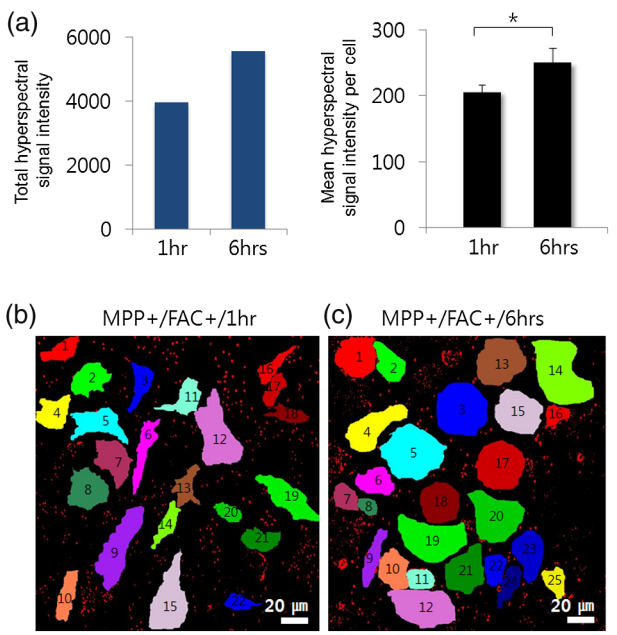

Fig. 6 Comparison of the total iron signal intensity (left) and mean iron signal intensity (right) between exposure time of 1 and 6 h (a). The regions of interest (ROIs) analyzed are shown in the hyperspectral iron signal image of (b) (1 h) and (c) (6 h).

In further studies, we will investigate what transporting pathway is mainly related to cellular uptake of iron in the cellular PD model. The extracellular iron can be transported into the cell via iron transporting proteins such as divalent metal transporter 1, ferroportin 1, transferrin receptor, and these transporters were upregulated in the PD models.[9,20,21] Intracellular iron uptakes and overloads might be correlated with overexpression of these proteins. Therefore, the colocalization study of various iron transporters and cellular iron mapped using hyperspectral fluorescence signal imaging will give a better understanding of the pathophysiological processes in PD progression.

4 Conclusion

This study demonstrated that iron particles move into dopaminergic cells in an MPP+-induced cellular model of PD. Nanoscale dark-field optical microscopy clearly showed the cellular deposition of iron and its subcellular location. Iron particles were dispersed as small, particulate forms in the cytosol. In shrunken cells, the particles were found to be concentrated at the cell membrane/edge. Our iron imaging methods can be applied to analyze the pathophysiological role of iron in PD. The application of this method might further be expanded to various neurological disorders that involve other metals, such as copper, manganese, or zinc.

Acknowledgments

This work was supported by Seoul National University Bundang Hospital (02-2005-027) and the Research Center

Program of the IBS (Institute for Basic Science) in South Korea. Author contributions: E.S.O., C.H., and J.M.K. designed the experiment; E.S.O. and C.H. performed experiments and analyzed the data; E.S.O., C.H., M.S., Y.H.L., and J.M.K. wrote the paper.

References

1. P. T. Lieu et al., "The roles of iron in health and disease," *Mol. Aspects Med.* **22**(1), 1–87 (2001).
2. E. Sofic et al., "Selective increase of iron in substantia nigra zona compacta of Parkinsonian brains," *J. Neurochem.* **56**(3), 978–982 (1991).
3. P. Damier et al., "The substantia nigra of the human brain. I. Nigrosomes and the nigral matrix: a compartmental organization based on calbindin D(28K) immunohistochemistry," *Brain* **122**(8), 1421–1436 (1999).
4. D. H. Kwon et al., "Seven-Tesla magnetic resonance images of the substantia nigra in Parkinson disease," *Ann. Neurol.* **71**(2), 267–277 (2012).
5. D. Berg et al., "Echogenicity of the substantia nigra: association with increased iron content and marker for susceptibility to nigrostriatal injury," *Arch. Neurol.* **59**(6), 999–1005 (2002).
6. A. H. Koeppen, "The history of iron in the brain," *J. Neurol. Sci.* **134**(134 Suppl), 1–9 (1995).
7. R. R. Crichton, D. T. Dexter, and R. J. Ward, "Brain iron metabolism and its perturbation in neurological diseases," *J. Neural. Transm.* **118**(3), 301–314 (2011).
8. L. Zecca et al., "Iron, brain ageing and neurodegenerative disorders," *Nat. Rev. Neurosci.* **5**(11), 863–873 (2004).
9. S. V. Kalivendi et al., "1-Methyl-4-phenylpyridinium (MPP+)-induced apoptosis and mitochondrial oxidant generation: role of transferrin-receptor-dependent iron and hydrogen peroxide," *Biochem. J.* **371**(1), 151–164 (2003).
10. J. Riemer et al., "Colorimetric ferrozine-based assay for the quantitation of iron in cultured cells," *Anal. Biochem.* **331**(2), 370–375 (2004).
11. K. Tulpule et al., "Uptake of ferrous iron by cultured rat astrocytes," *J. Neurosci. Res.* **88**(3), 563–571 (2010).
12. Y. Garini, B. J. Vermolen, and I. T. Young, "From micro to nano: recent advances in high-resolution microscopy," *Curr. Opin. Biotechnol.* **16**(1), 3–12 (2005).
13. A. Vainrub, O. Pustovyy, and V. Vodyanoy, "Resolution of 90 nm (lambda/5) in an optical transmission microscope with an annular condenser," *Opt. Lett.* **31**(19), 2855–2857 (2006).
14. A. Nair et al., "Enhanced intratumoral uptake of quantum dots concealed within hydrogel nanoparticles," *Nanotechnology* **19**(48), 485102 (2008).
15. K. Sarlo et al., "Tissue distribution of 20 nm, 100 nm and 1000 nm fluorescent polystyrene latex nanospheres following acute systemic or acute and repeat airway exposure in the rat," *Toxicology* **263**(2), 117–126 (2009).
16. J. N. Meyer et al., "Intracellular uptake and associated toxicity of silver nano particles in Caenorhabditis elegans," *Aquat. Toxicol.* **100**(2), 140–50 (2010).
17. T. Dučić et al., "X-ray fluorescence analysis of iron and manganese distribution in primary dopaminergic neurons," *J. Neurochem.* **124**(2), 250–261 (2013).
18. R. Ortega et al., "Iron storage within dopamine neurovesicles revealed by chemical nano-imaging," *PLoS One* **2**(9), e925 (2007).
19. D. Berg and H. Hochstrasser, "Iron metabolism in Parkinsonian syndromes," *Mov. Disord.* **21**(9), 1299–1310 (2006).
20. J. Salazar et al., "Divalent metal transporter 1 (DMT1) contributes to neurodegeneration in animal models of Parkinson's disease." *Proc. Natl. Acad. Sci. U. S. A.* **105**(47), 18578–18583 (2008).
21. N. Song et al., "Ferroportin1 and hephaestin overexpression attenuate iron-induced oxidative stress in MES23.5 dopaminergic cells," *J. Cell. Biochem.* **110**(5), 1063–1072 (2010).